

# Thermodynamic Properties of Difluoromethane

Dana R. Defibaugh,\* Graham Morrison, and Lloyd A. Weber

Thermophysics Division, Chemical Science & Technology Laboratory, National Institute of Standards and Technology, Gaithersburg, Maryland 20899

The pressure-volume-temperature (PVT) behavior of difluoromethane (R32) has been measured using a vibrating tube densimeter apparatus and a Burnett/isochoric apparatus. Liquid PVT data from the vibrating tube densimeter ranged in temperature from 242 to 348 K with a pressure range of 2000-6500 kPa. Data from the Burnett apparatus consisted of 11 isochores for the gas and supercritical fluid, along with vapor pressure measurements. The temperature ranged from 268 to 373 K. The gas-phase data are correlated with a virial equation of state. The compressed liquid data are fit with an abbreviated form of the modified Benedict-Webb-Rubin (mBWR) equation. A table of thermodynamic properties is presented for the saturated liquid and vapor states.

## Introduction

Chlorofluorocarbons (CFC) and hydrochlorofluorocarbons (HCFC) have been implicated as the cause of ozone depletion in the stratosphere (1). The Montreal Protocol prescribes a schedule for phasing out the production of CFCs and HCFCs around the world. The phasing out of environmentally harmful refrigerants forces us to consider alternatives that can perform as well or better than CFCs or HCFCs. Mixtures containing the alternative refrigerant difluoromethane (R32) are being considered as replacements for chlorodifluoromethane (R22), and for the azeotropic mixture (R502) of R22 and chloropentafluoroethane (R115). Calculation of the thermophysical properties of mixtures requires reliable data for the properties of the pure components. Difluoromethane is an especially interesting fluid because of its large dipole moment (1.98 D) (2). Therefore, it is important to know the thermophysical properties of pure R32 accurately in order that the properties of its mixtures can be accurately modeled. We have measured gas-phase and liquid-phase pressure-volume-temperature (PVT) data as well as vapor pressures for R32.

## Apparatus and Procedure

Difluoromethane (R32) was supplied by E. I. duPont deNemours, Inc. (3), with a stated purity of 99.99 wt %. Gas chromatographic analysis of the sample was consistent with the manufacturer's analysis (4). No further analysis or purification of the sample was conducted.

**A. Burnett Apparatus.** The Burnett apparatus has been thoroughly documented in earlier publications (5-7), and is only briefly described here. The sample cell of the Burnett apparatus was composed of a heavy-walled nickel vessel with two gold-plated inner chambers. The ratio of the volumes of the inner chambers was  $1.782\ 06 \pm 0.000\ 07$  (1 $\sigma$ ). The chambers were connected to a sensitive, diaphragm-type pressure transducer (5) through a small tube. The transducer separated the sample from an external, argon-filled manifold in which the argon pressure was balanced against the sample pressure using an automated, piston-type gas injector. The manifold pressure was measured with a Ruska quartz spiral bourdon pressure gauge and a Ruska dead weight gauge (3). Pressure could be measured with an uncertainty of  $\pm 0.01$  kPa. The Burnett apparatus was mounted in a circulating thermostated oil bath. The temperature of the bath was

measured with a platinum resistance thermometer (PRT) with an uncertainty of  $\pm 0.002$  K. A feedback circuit using the thermometer, an ac bridge, a signal conditioner, and a programmable power supply controlled the temperature of the oil bath. A second PRT measured the temperature of the sample vessel. In the automatic mode, which was used for data acquisition on isochores, a microcomputer set the desired temperature, monitored equilibration, and measured temperature and pressure. The automatic mode was also used for measuring vapor pressures. For the Burnett expansion data on the isotherms at 373.124 K, the pressure was measured with a manually operated dead weight pressure balance. The uncertainty of the dead weight gauge pressure measurements was on the order of  $\pm 0.01$  kPa. The Burnett expansion mode was used to determine the density as a function of pressure on the isotherm 373.124 K. Thereafter, the pressure was measured as a function of temperature on isochores. All temperatures are given on the ITS-90 scale.

**B. Densimeter.** A stainless steel vibrating tube densimeter was used to measure compressed liquid densities. The apparatus has a liquid volume of 3.5 cm<sup>3</sup>; the vibrating tube is made of stainless steel with a wall thickness of 0.3 mm and an inside diameter of 2.4 mm. The densimeter apparatus is accurate to  $\pm 0.0005$  g/cm<sup>3</sup>. The densimeter has been thoroughly discussed in an earlier publication (8); a brief description is given here. The temperature of the densimeter was regulated by a thermostated circulating bath. A water/ethylene glycol solution was circulated through a heat exchanger surrounding the vibrating tube at temperatures above 273.15 K. At temperatures below 273.15 K, methanol was used in the circulating bath. The heat exchanger surrounding the vibrating tube was enclosed in a temperature-controlled air bath maintained at the same temperature. A platinum resistance thermometer monitored the temperature of the liquid exiting the heat exchanger. Temperatures (ITS-90) are accurate to  $\pm 0.01$  K.

A manifold located outside the air bath consisted of mercury reservoirs and a mercury manometer/separator. A glass capillary in the manometer/separator allowed us to locate the mercury level in the manometer, which separated the refrigerant sample from pressurizing argon gas. The pressure of the system was maintained above the vapor pressure of R32 in the vibrating tube at temperatures above ambient. When the vibrating tube was below room temperature, the lower pressure limit was determined by the vapor pressure of R32 at the temperature of the manometer. The pressure

\* To whom all correspondence should be addressed.

**Table 1. Burnett/Isotherm Data for R32 (Difluoromethane)**

<i>T</i> /K	$\rho$ /(mol·dm <sup>-3</sup> )	<i>P</i> /kPa	<i>T</i> /K	$\rho$ /(mol·dm <sup>-3</sup> )	<i>P</i> /kPa
373.130	2.558 30	5258.13	373.128	0.079 88	244.57
373.130	2.558 30	5257.97	373.135	10.603 10	9773.46
373.130	1.435 61	3520.45	373.136	5.949 90	7727.70
373.129	1.435 61	3520.85	373.134	3.338 80	6105.08
373.131	0.805 59	2188.83	373.137	1.873 50	4283.26
373.139	0.805 59	2188.82	373.133	1.051 33	2742.89
373.134	0.452 06	1301.85	373.132	0.589 96	1660.47
373.133	0.452 06	1302.05	373.129	0.331 06	972.58
373.133	0.253 67	754.91	373.131	0.185 77	559.05
373.132	0.253 67	755.16	373.130	0.104 25	317.92
373.130	0.142 35	431.51			

of the argon was monitored with a quartz pressure transducer. The pressures were accurate to  $\pm 0.5$  kPa. Before a sample was loaded, the apparatus was rinsed with ethanol and then acetone to remove any residue from previous experiments. Once the apparatus was filled, compressed liquid densities for R32 were measured. The resulting measurements were recorded by computer. The temperature and pressure of the densimeter were monitored by the computer and changed after each measurement was completed.

## Results

**A. Burnett Measurements.** Burnett expansion measurements were made at 373.124 K. Sixteen pressures were measured in two separate runs totaling 14 expansions ranging in density from 0.12 to 10.6 mol/dm<sup>3</sup>. Results are given in Table 1. After the pressure–density relationship was established on the 373.124 K isotherm, data were collected on isochores. A total of 146 data were collected along 11 isochores between the temperatures of 268 and 373 K. The pressure measurement for each isochore at 373.124 K was used to determine the density. A temperature correction to the densities was made to compensate for the thermal expansion of the sample cell. The Burnett expansion data at 373.124 K with densities less than 1.05 mol/dm<sup>3</sup> (2.74 MPa) were analyzed with a two-term virial equation. The standard deviation of the fit was 0.19 kPa, and the virial coefficients had the values  $B = -0.164\ 36 \pm 0.000\ 50$  dm<sup>3</sup>/mol and  $C = 0.012\ 39 \pm 0.000\ 75$  dm<sup>6</sup>/mol<sup>2</sup>. The densities for higher pressure data were calculated using the cell constant, and then all of the data were fit with a polynomial so that they could be interpolated to calculate the densities where the isochores intersected the Burnett isotherm. Results of the isochoric measurements are given in Table 2 and are reported in the same order as the data were collected.

All of the data having densities less than 2.56 mol/dm<sup>3</sup> were represented with a three-term virial surface:

$$\frac{PV}{RT} = 1 + \frac{B}{V} + \frac{C}{V^2} + \frac{D}{V^3} \quad (1)$$

$$B = B_0 + B_1 T_r^{-1} + B_2 T_r^{-2} + B_3 T_r^{-3} + B_4 T_r^{-6} + B_5 T_r^{-8}$$

$$C = C_0 T_r^{-5} + C_1 T_r^{-6} \quad (2)$$

$$D = D_0 + D_1 T_r$$

$B_0 = 0.373\ 714\ 54$	$C_0 = 0.053\ 860\ 69$
$B_1 = -0.929\ 075\ 48$	$C_1 = -0.035\ 904\ 1$
$B_2 = 0.603\ 192\ 842\ 8$	$D_0 = -0.002\ 690\ 2$
$B_3 = -0.223\ 258\ 04$	$D_1 = 0.001\ 981\ 68$
$B_4 = -0.020\ 098\ 19$	$T_c = 351.36\ \text{K}$
$B_5 = 0.001\ 029\ 230$	$T_r = T/T_c$
	$R = 0.083\ 144\ 5\ \text{J K}^{-1}\ \text{mol}^{-1}$

The values of  $B$  and  $C$  at 373.124 K for this surface are  $-0.1656$

dm<sup>3</sup>/mol and 0.0143 dm<sup>6</sup>/mol<sup>2</sup>, respectively. To improve the reliability of the surface at low temperatures, we included in the fit, with a low weight, the values for the second virial coefficient estimated by Weber and Goodwin (9). A comparison of this surface with our own PVT data and with those of Qian et al. (10) in this density range is shown in Figure 1. The data of Qian et al. (10) deviate systematically from the surface by an average of 0.25%. Most of our data are represented well by the surface; however, the two lowest density isochores also have rather large positive systematic deviations at low temperatures. The isochores having densities of 0.14 and 0.25 mol/dm<sup>3</sup> have average deviations of 0.28% and 0.12%, respectively, at temperatures below 320 K. The remainder of our data are fit with a standard deviation of 0.037%.

The sign of the deviations of the lowest density isochores is such that they could be caused by physical adsorption of sample on the walls of the cell. Such behavior would not be surprising in view of the large dipole moment of the R32 molecules. No reasonable adjustment of the virial coefficients could reduce these deviations. For this reason, we believe that the surface given by eq 1 provides a better estimate of the vapor densities of R32 than either our own data or those from ref 10.

The Burnett apparatus was also used to measure vapor pressures. Pressure measurements on isochores inside the two-phase region yielded vapor pressures. The 18 vapor pressure measurements given in Table 3 were collected in the range 268–348 K. These data were measured on the isochores having nominal densities of 10.6 and 2.56 mol/dm<sup>3</sup>. The good agreement between the data at two very different densities is consistent with the high purity of the sample. The present vapor pressure data were combined with the ebulliometric data of Weber and Goodwin (9) which range in temperature from 208 to 237 K and also with the unpublished results of Weber and Silva (11) between 235 and 265 K. The combined data set was correlated with the following equation:

$$\ln P = \ln P_c + (T_c/T)[x_1 \tau + x_2 \tau^{1.5} + x_3 \tau^{2.5} + x_4 \tau^5] \quad (3)$$

$x_1 = -7.459\ 598\ 6$	$\tau = 1 - T/T_c$
$x_2 = 1.734\ 032\ 0$	$P_c = 5792.7\ \text{kPa}$
$x_3 = -1.994\ 149\ 4$	$T_c = 351.36\ \text{K}$
$x_4 = -2.532\ 926\ 3$	

Equation 3 fits the data with a relative standard deviation of 0.028% in pressure. The critical temperature was fixed at the value measured by Schmidt and Moldover (12) (351.36 K). The critical pressure, which was an adjustable parameter in the correlation, was found to be 5792.7 kPa with an uncertainty of  $\pm 2.4$  kPa. Figure 2 shows the relative deviation of the data in Table 3 from eq 3 as well as the data of Weber and Goodwin (9), Malbrunot et al. (13), and Weber and Silva (11).

The saturated vapor densities were determined by substituting the equilibrium vapor pressure calculated from eq 3 and the temperature into the virial equation of state, eq 1. The saturated vapor densities and pressures are listed in Table 4.

**B. Densimeter Measurements.** Compressed-liquid-density measurements for R32 were made along 22 isotherms at pressures from 2000 to 6500 kPa. The densities, listed in Table 5, span values from 12 to 22 mol/dm<sup>3</sup>. Isotherms of the compressed liquid were extrapolated to the saturation boundary using the Tait (14) equation to determine the saturation densities. Coefficients for the Tait extrapolations can be furnished upon request. Above room temperature the measurements at the lowest pressure were close to the saturation boundary; however, at the lowest temperature,

Table 2. Burnett/Isochoric PVT Data for R32 (Difluoromethane)

T/K	$\rho/(\text{mol}\cdot\text{dm}^{-3})$	P/kPa	T/K	$\rho/(\text{mol}\cdot\text{dm}^{-3})$	P/kPa	T/K	$\rho/(\text{mol}\cdot\text{dm}^{-3})$	P/kPa	T/K	$\rho/(\text{mol}\cdot\text{dm}^{-3})$	P/kPa
338.104	2.561 01	4090.31	363.120	0.452 25	1259.9	283.164	0.254 63	547.224	353.111	5.954 90	5930.64
343.118	2.560 47	4265.14	358.128	0.452 34	1238.99	278.129	0.254 68	534.892	358.095	5.953 66	6387.23
348.125	2.559 94	4436.54	353.130	0.452 44	1217.88	273.143	0.254 74	522.559	363.135	5.952 40	6840.92
353.095	2.559 40	4603.931	348.152	0.452 53	1196.78	268.916	0.254 78	512.057	368.142	5.951 15	7286.73
358.084	2.558 87	4769.34	343.144	0.452 62	1175.37	268.834	0.254 78	511.840	373.145	5.949 89	7728.75
363.143	2.558 32	4934.86	338.128	0.452 72	1154.47	368.109	0.142 38	425.416	343.151	3.343 00	4724.23
368.129	2.557 79	5096.09	333.118	0.452 82	1132.15	363.120	0.142 41	419.294	348.130	3.342 31	4964.34
373.143	2.557 25	5256.39	328.073	0.452 91	1110.44	358.130	0.142 44	413.125	353.117	3.340 61	5199.12
363.119	2.558 32	4934.19	323.186	0.453 00	1089.37	358.130	0.142 44	413.125	353.117	3.341 61	5199.12
363.129	2.558 32	4934.42	318.156	0.453 10	1067.23	353.126	0.142 50	400.884	363.135	3.340 20	5658.67
368.103	1.435 91	3441.3	313.101	0.453 20	1044.79	348.126	0.142 50	400.884	363.135	3.340 20	5658.67
363.121	1.436 21	3361.93	308.158	0.453 29	1022.66	343.157	0.142 53	394.770	368.142	3.339 50	5883.66
358.124	1.436 51	3281.77	303.140	0.453 38	999.969	338.080	0.142 56	388.492	373.086	3.338 81	6103.12
353.128	1.436 82	3200.72	298.125	0.453 48	977.073	333.070	0.142 59	382.250	328.222	1.877 03	3255.45
348.159	1.437 12	3119.25	293.172	0.453 57	954.2209	323.130	0.142 62	376.086	333.082	1.876 65	3373.69
343.139	1.437 42	3036.07	288.132	0.453 67	930.6519	323.130	0.142 65	369.874	338.103	1.876 26	3493.40
338.132	1.437 72	2952.06	283.166	0.453 76	907.07	323.175	0.142 65	369.837	343.124	1.875 86	3611.04
333.119	1.438 02	2866.77	323.155	0.453 00	1089.22	323.148	0.142 65	369.777	348.141	1.875 47	3726.92
323.130	1.438 63	2692.81	278.145	0.453 86	882.259	323.155	0.142 65	369.793	353.120	1.875 07	3840.35
318.099	1.438 93	2602.63	281.187	0.453 80	897.138	323.150	0.142 65	369.831	358.145	1.874 68	3953.46
372.446	1.435 65	3509.56	368.110	0.253 73	743.814	318.110	0.142 68	363.448	363.133	1.874 29	4064.42
372.442	1.435 65	3509.64	363.170	0.253 78	732.777	313.112	0.142 71	357.156	368.140	1.873 89	4174.68
368.109	0.805 76	2149.14	358.133	0.253 83	721.402	308.155	0.142 74	350.916	373.142	1.873 50	4283.79
363.115	0.805 93	2108.95	353.133	0.253 89	710.161	303.133	0.142 77	344.557	308.164	1.054 20	1994.00
358.120	0.806 10	2068.62	348.155	0.253 94	698.929	298.176	0.142 80	338.316	313.138	1.053 98	2055.91
353.127	0.806 26	2027.99	343.140	0.253 99	687.532	293.144	0.142 83	331.853	318.131	1.053 76	2116.95
348.163	0.806 43	1987.31	338.129	0.254 05	676.108	288.154	0.142 86	325.478	323.145	1.053 54	2177.34
343.100	0.806 60	1945.35	333.121	0.254 10	664.666	283.161	0.142 89	319.180	328.145	1.053 32	2236.59
338.134	0.806 77	1904.01	328.063	0.254 15	653.053	278.146	0.142 92	312.783	333.148	1.053 10	2295.19
333.165	0.806 94	1862.22	322.930	0.254 21	641.187	273.158	0.142 95	306.300	338.150	1.052 87	2353.09
328.057	0.806 11	1818.84	318.138	0.254 26	629.987	268.530	0.142 97	300.240	343.109	1.052 66	2409.88
323.135	0.807 28	1776.45	313.161	0.254 31	618.430	268.133	0.142 98	299.730	348.136	1.052 43	2466.83
318.143	0.807 45	1733.15	308.156	0.254 37	606.736	353.110	10.608 3	6145.060	353.108	1.052 21	2522.64
313.168	0.807 62	1689.48	303.138	0.254 42	594.911	358.089	10.606 1	7014.010	358.138	1.051 99	2578.58
308.177	0.807 78	1645.0	298.122	0.254 47	583.077	363.132	10.603 8	7921.320	363.131	1.051 77	2633.75
323.084	0.807 28	1776.22	293.167	0.254 53	571.318	368.149	10.601 6	8842.059	368.139	1.051 55	2688.66
368.106	0.452 15	1280.8	288.191	0.254 58	559.386	373.131	10.599 4	9769.821	373.141	1.051 33	2743.05

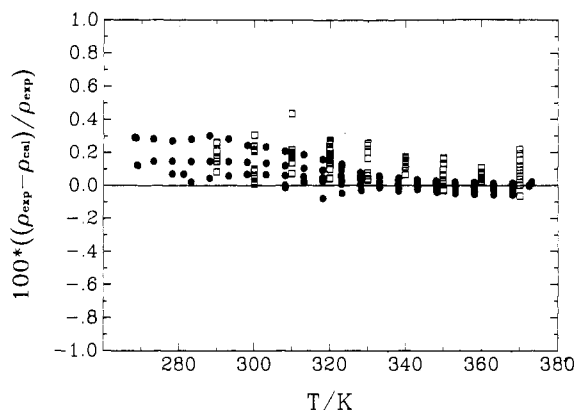


Figure 1. Density difference from eq 1 of this work (●) and the data of Qian et al. (10) (□).

Table 3. Burnett Vapor Pressures for R32

T/K	P/kPa	T/K	P/kPa
268.154	690.56	313.122	2476.63
273.163	813.62	318.154	2794.65
278.137	951.22	318.169	2795.42
283.184	1108.22	323.161	3140.65
288.129	1280.21	328.202	3522.52
293.121	1473.50	333.105	3927.61
298.174	1690.81	338.150	4382.59
303.122	1926.26	343.110	4871.98
308.143	2189.50	348.081	5409.01

the extrapolation extends over 1000 kPa. However, nearly linear behavior of density with pressure at the lowest temperatures leaves the extrapolation relatively free of systematic errors. The saturation pressure for the extrapolation was calculated from eq 3. The saturated liquid

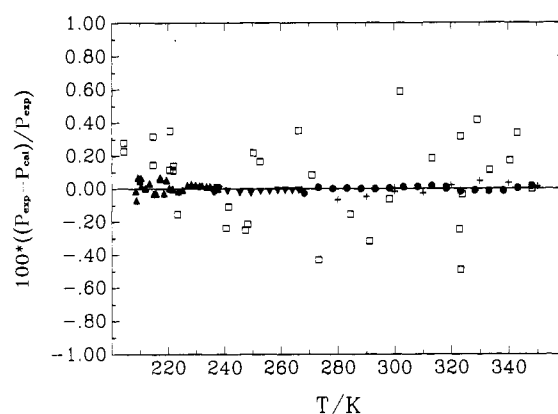


Figure 2. Pressure difference from eq 3 of this work (●), the data of Weber and Goodwin (9) (▲), the data of Malbrunot et al. (13) (□), the data of Weber and Silva (11) (▼), and the data of Qian et al. (10) (△).

densities are listed in Table 6. The saturated liquid densities were fit with the following function:

$$\rho/(\text{mol}\cdot\text{dm}^{-3}) = \rho_c + \chi(\rho_1 + \rho_2\chi + \rho_3\chi^2 + \rho_4\chi^3) \quad (4)$$

$$\begin{aligned} \rho_c &= 8.1247 \text{ mol/dm}^3 & \chi &= (351.36 - T/\text{K})^{1/3} \\ \rho_1 &= 2.214 664 9 \\ \rho_2 &= 0.138 835 22 \\ \rho_3 &= -5.537 487 6 \times 10^{-3} \\ \rho_4 &= 1.761 141 1 \times 10^{-3} \end{aligned}$$

The value of  $\rho_c$  was taken from Niesen et al. (15). Equation 4 represents the measured saturated liquid densities within  $\pm 0.002 \text{ mol/dm}^3$ , well within the estimated uncertainty of these densities (see Figure 3.)

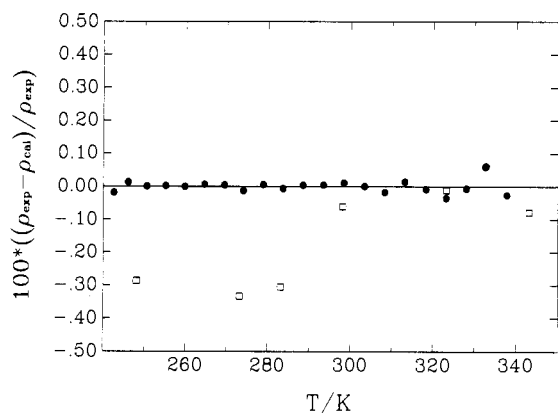


**Figure 3.** Difference of measured saturated liquid densities from eq 4 of this work (●) and the data of Malbrunot et al. (13) (□).

**Table 4. Burnett Saturated Vapor Densities for R32 (Difluoromethane)**

T/K	P/kPa	$\rho$ /(mol·dm <sup>3</sup> )	T/K	P/kPa	$\rho$ /(mol·dm <sup>3</sup> )
219	89.09	0.0509	289	1312.4	0.6941
224	114.93	0.0647	294	1509.7	0.8054
229	146.41	0.0813	299	1728.4	0.9326
234	184.35	0.1010	304	1970.2	1.0785
239	229.62	0.1244	309	2236.7	1.2466
244	283.15	0.1519	314	2529.6	1.4414
249	345.91	0.1840	319	2850.8	1.6690
254	418.93	0.2214	324	3202.3	1.9385
259	503.27	0.2645	329	3586.5	2.2631
264	600.05	0.3142	334	4005.9	2.6649
269	710.42	0.3713	336	4184.3	2.8552
274	835.58	0.4367	339	4463.9	3.1841
279	976.77	0.5114	340	4560.4	3.3084
284	1135.2	0.5967	343	4860.4	3.7403

The compressed liquid densities and saturated liquid densities were correlated with an abbreviated mBWR (16) equation of state, given by eq 5. The temperature dependence

$$P = \sum_{n=1}^3 a_n(T) \rho^n + e^{-(\rho/\rho_c)^2} \sum_{n=4}^9 a_n(T) \rho^{2n-5} \quad (5)$$

of the coefficients is given by

$$\begin{aligned} a_1 &= RT \\ a_2 &= b_1 T + b_2 T^{0.5} + b_3 + b_4 / T + b_5 T^2 \\ a_3 &= b_6 T + b_7 + b_8 / T + b_9 / T^2 \\ a_4 &= b_{10} / T^2 + b_{11} / T^3 \\ a_5 &= b_{12} / T^2 + b_{13} / T^4 \\ a_6 &= b_{14} / T^2 + b_{15} / T^3 \\ a_7 &= b_{16} / T^2 + b_{17} / T^4 \\ a_8 &= b_{18} / T^2 + b_{19} / T^3 \\ a_9 &= b_{20} / T^2 + b_{21} / T^3 + b_{22} / T^4 \end{aligned} \quad \begin{aligned} T_c &= 351.36 \text{ K} \\ \rho_c &= 8.1247 \text{ mol/L} \\ R &= 0.0831445 \text{ J K}^{-1} \text{ mol}^{-1} \\ \text{MW} &= 52.023 \text{ g} \cdot \text{mol}^{-1} \end{aligned}$$

The coefficients obtained from the linear least-squares fit of the abbreviated mBWR to the thermodynamic surface of R32 are

$$\begin{aligned} b_1 &= 60.5857348602845 & b_{12} &= 79745.0579332389 \\ b_2 &= -4246.73061580673 & b_{13} &= 24609.0305215865 \\ b_3 &= 88614.5462673095 & b_{14} &= 10753.9337004544 \\ b_4 &= -17039.0212577371 & b_{15} &= -3886441.99147113 \\ b_5 &= 1838304373.81754 & b_{16} &= 2.00310213358674 \\ b_6 &= 0.595590535169489 & b_{17} &= 2.43556218395226 \\ b_7 &= -645.366934591639 & b_{18} &= 0.110156331238649 \\ b_8 &= 346460.239800627 & b_{19} &= -57.7740264191463 \\ b_9 &= -49776.0045697313 & b_{20} &= -9.54420104215448 \times 10^{-5} \\ b_{10} &= 231787076.777383 & b_{21} &= 0.140429980815947 \\ b_{11} &= -57742159354.7545 & b_{22} &= -19.7451529232523 \end{aligned}$$

This equation was selected as a convenient means of correlating the liquid properties of this fluid and was used for comparison between 220 and 350 K and from the saturation pressure to 7000 kPa. Equation 5 is not an appropriate representation of R32 outside this temperature and pressure region. Equation (5) represents the data to  $\pm 0.01\%$  in density except near the critical point where the deviations rise to  $\pm 0.15\%$  at 348 K. Larger deviations occur as you approach the critical temperature point of the fluid. The larger deviation is attributed to the inadequacy of the mBWR equation to model highly curved isotherms in the critical region where the true equation of state has a nonanalytic character. Figure 4 shows the density deviation of the present data and of the data of Malbrunot (13) and Qian (10) from eq 5.

**C. Thermodynamic Properties.** In the previous sections of this paper we have discussed the experimental determination of the PVT properties of R32, both as a gas and as a compressed liquid, over a wide set of conditions. We have also described measurement of the vapor pressure from 268 to 348 K, which, when combined with the earlier measurements of Weber and Goodwin (9), and with those of Weber and Silva (11), allowed us to represent the vapor pressure of R32 from below the normal boiling point (221.49 K) to the critical point (351.36 K). The conditions spanned by these data are displayed in Figures 5 and 6.

These data combined with the ideal gas properties allow one to evaluate other thermodynamic properties, such as the heat capacities, enthalpies, and entropies.

The results of these calculations appear in Tables 7–10. The tables begin at 220 K, slightly below the normal boiling point and below the lowest temperature for which we made liquid or vapor PVT measurements. The entries arise from the virial equation of state and its extrapolation, the correlation of the saturated liquid densities and its extrapolation, and the derivatives  $(\partial P/\partial T)_\rho$  and  $(\partial V/\partial T)_\rho$ , for the saturated liquid states. Values of these derivatives were determined from direct numerical differentiation of the data for the compressed liquid states without any reference to a correlation of the liquid PVT data. The values below 242 K were data obtained by extrapolation with a quadratic function of  $T$ .

Table 7 gives the ideal gas properties from 200 to 400 K. The reference state for the entropy and the enthalpy in this table is the ideal gas at 101.325 kPa and 233.15 K. The ideal gas enthalpy is not a function of pressure or volume. The ideal gas entropy at the pressure or volume of the saturated vapor relative to the reference state described here can be evaluated by making the usual corrections,  $R \ln(101.325/P)$  for pressure and  $R \ln(101.325V/RT)$  for volume. The pressure (kPa) and volume (dm<sup>3</sup>/mol) are the experimental values for the saturated vapor. The contribution of the vibrational modes to these properties was calculated from the normal mode frequencies measured by Suzuki and Shimanouchi (17). No corrections for anharmonicities were made because the least energetic of these modes has an equivalent temperature of 760 K and is substantially above the temperatures represented in the table and because the next least energetic mode has a temperature of 1568 K. An error of 0.5 cm<sup>-1</sup> in each of the vibrational modes gives rise to an error of no more than 0.01 J mol<sup>-1</sup> K<sup>-1</sup> in the heat capacity, 0.002 J mol<sup>-1</sup> K<sup>-1</sup> in the entropy, and 0.5 J mol<sup>-1</sup> in the enthalpy. The vibrational contribution to these properties at 233.15 K with respect to the ground-state properties at 0.0 K is noted at the end of the table. No contribution to the entropy due to the symmetry of the molecule has been included in the final entry.

Table 8 gives the properties of the saturated vapor from 220 to 340 K with a separate entry for the critical temperature. The reference state for this table is the saturated liquid at

**Table 5. Densimeter PVT Data for R32 (Difluoromethane)**

T/K	$\rho/(\text{mol}\cdot\text{dm}^{-3})$	P/kPa	T/K	$\rho/(\text{mol}\cdot\text{dm}^{-3})$	P/kPa	T/K	$\rho/(\text{mol}\cdot\text{dm}^{-3})$	P/kPa	T/K	$\rho/(\text{mol}\cdot\text{dm}^{-3})$	P/kPa
242.593	22.244	1999.2	264.505	21.078	4501.9	293.459	18.901	2000.4	323.110	16.626	5003.4
242.596	22.265	2499.3	264.520	21.105	5002.5	293.459	18.955	2500.3	323.109	16.734	5503.7
242.582	22.287	3001.3	264.518	21.132	5503.0	293.460	19.007	3001.4	323.111	16.835	6003.6
242.584	22.307	3501.1	264.511	21.160	6002.9	293.459	19.058	3501.5	323.111	16.931	6504.5
242.582	22.328	4001.0	264.524	21.186	6503.8	293.464	19.108	4001.2	327.960	15.689	3802.5
242.588	22.348	4502.0	269.378	20.622	2000.3	293.463	19.156	4502.2	327.962	15.757	4001.8
242.586	22.368	5002.3	269.382	20.654	2500.7	293.462	19.204	5003.0	327.962	15.917	4502.6
242.594	22.388	5502.2	269.381	20.685	3000.9	293.458	19.251	5503.4	327.964	16.062	5003.5
242.588	22.408	6002.1	269.387	20.716	3501.1	293.461	19.296	6003.3	327.963	16.195	5503.8
242.592	22.427	6503.0	269.397	20.747	4001.1	293.461	19.341	6504.2	327.968	16.319	6003.6
246.019	22.047	2000.8	269.398	20.777	4502.1	298.407	18.494	2000.4	327.964	16.434	6504.5
246.022	22.069	2499.9	269.397	20.807	5003.0	298.409	18.555	2500.4	332.789	15.089	4202.3
246.033	22.090	3000.9	269.400	20.837	5503.0	298.419	18.614	3001.4	332.795	15.219	4502.7
246.053	22.111	3501.2	269.393	20.867	6003.1	298.415	18.672	3501.4	332.800	5.415	5003.4
246.061	22.132	4000.8	269.396	20.896	6503.8	298.417	18.728	4001.3	332.799	15.588	5503.8
246.064	22.153	4502.1	273.999	20.315	2000.3	298.419	18.782	4502.3	332.799	15.745	6003.6
246.077	22.173	5002.9	274.003	20.350	2500.6	298.426	18.835	5003.1	332.800	15.888	6504.4
246.091	22.193	5503.2	274.003	20.384	3000.9	298.424	18.887	5503.3	337.788	14.291	4503.0
246.108	22.213	6003.1	274.004	20.418	3501.6	298.426	18.937	6003.2	337.792	14.597	5003.4
246.102	22.234	6503.9	274.008	20.452	4001.2	303.424	18.122	2501.3	337.793	14.847	5503.7
250.554	21.783	2000.6	274.007	20.485	4502.2	303.428	18.191	3001.4	337.790	15.060	6003.5
250.569	21.806	2500.7	274.010	20.518	5003.0	303.425	18.258	3501.6	337.792	15.248	6504.4
250.568	21.829	3000.8	274.005	20.550	5503.3	303.422	18.322	4001.5	347.638	13.564	6504.4
250.578	21.852	3501.1	274.008	20.581	6003.1	303.421	18.384	4502.4	347.675	12.540	5604.3
250.581	21.874	4001.2	274.011	20.613	6504.0	303.42	18.444	5003.1	347.701	12.827	5803.8
250.580	21.897	4501.9	278.812	19.988	2000.3	303.418	18.503	5503.5	347.682	13.073	6003.3
250.572	21.920	5002.9	278.813	20.026	2500.7	303.423	18.559	6003.2	347.659	13.285	6203.9
250.581	21.942	5503.2	278.816	20.064	3001.0	303.347	18.620	6504.2	347.603	13.473	6404.0
250.587	21.963	6003.0	278.827	20.101	3501.6	308.303	17.672	2501.1	347.562	13.564	6504.5
250.572	21.986	6503.9	278.827	20.137	4001.3	308.287	17.752	3001.3	348.530	11.646	5303.7
255.116	21.512	2000.4	278.833	20.173	4502.1	308.253	17.831	3501.5	348.537	11.733	5353.6
255.120	21.537	2500.8	278.835	20.208	5002.8	308.252	17.906	4001.4	348.568	11.673	5403.5
255.125	21.561	3001.1	278.828	20.244	5503.1	308.255	17.977	4502.3	348.569	11.808	5453.4
255.13	21.586	3501.2	278.822	20.278	6003.0	308.261	18.045	5003.2	348.592	11.924	5503.2
255.134	21.610	4000.8	278.815	20.313	6503.9	308.269	18.111	5503.4	348.608	12.032	5553.7
255.136	21.634	4501.9	283.647	19.646	2000.3	308.267	18.174	6003.3	348.601	12.142	5603.6
255.141	21.658	5002.7	283.647	19.688	2500.3	308.248	18.238	6504.2	348.599	12.244	5653.4
255.142	21.682	5503.1	283.647	19.730	3001.4	313.123	17.278	3001.7	348.600	12.340	5703.3
255.146	21.705	6003.2	283.647	19.771	3501.5	313.118	17.369	3501.6	348.605	12.429	5753.2
255.133	21.729	6503.9	283.647	19.811	4001.3	313.126	17.455	4001.3	348.622	12.511	5803.7
259.752	21.230	2000.6	283.642	19.851	4502.2	313.131	17.537	4502.3	348.629	12.583	5853.6
259.753	21.257	2500.7	283.641	19.890	5002.9	313.134	17.617	5003.1	348.567	12.672	5903.4
259.765	21.283	3000.9	283.643	19.928	5503.3	313.143	17.692	5503.5	348.578	12.747	5953.2
259.771	21.310	3501.3	283.643	19.966	6003.2	313.156	17.764	6003.3	348.567	12.817	6003.0
259.770	21.336	4001.0	283.643	20.003	6504.1	313.148	17.835	6504.2	348.568	12.880	6053.6
259.779	21.362	4502.2	288.527	19.285	2000.6	318.251	16.831	3502.3	348.577	12.938	6103.4
259.790	21.387	5002.8	288.530	19.332	2500.4	318.255	16.936	4001.7	348.584	12.994	6153.3
259.799	21.412	5503.2	288.533	19.378	3001.4	318.255	17.036	4502.6	348.601	13.044	6203.4
259.797	21.437	6003.0	288.526	19.424	3501.4	318.254	17.131	5003.5	348.611	13.093	6253.4
259.806	21.462	6503.9	288.529	19.469	4001.2	318.253	17.221	5503.8	348.609	13.145	6304.1
264.487	20.935	2000.5	288.529	19.512	4502.1	318.253	17.306	6003.7	348.607	13.193	6354.0
264.488	20.964	2500.5	288.531	19.555	5003.0	318.251	17.389	6504.5	348.595	13.244	6403.9
264.501	20.993	3000.9	288.529	19.597	5503.5	323.107	16.255	3502.4	348.604	13.289	6453.9
264.506	21.021	3501.5	288.532	19.638	6003.3	323.110	16.388	4001.7	348.595	13.335	6503.9
264.528	21.049	4001.1	288.531	19.679	6504.2	323.110	16.511	4502.7			

**Table 6. Densimeter Saturated Liquid Densities for R32 (Difluoromethane)**

T/K	P/kPa	$\rho/(\text{mol}\cdot\text{dm}^{-3})$	T/K	P/kPa	$\rho/(\text{mol}\cdot\text{dm}^{-3})$
242.589	267.1	22.168	293.461	1487.4	18.845
246.063	307.9	21.974	298.418	1701.8	18.457
250.574	367.7	21.706	303.414	1940.7	18.044
255.132	437.0	21.433	308.266	2196.0	17.620
259.778	517.5	21.148	313.135	2477.0	17.178
264.509	610.6	20.853	318.253	2801.0	16.670
269.391	719.7	20.539	323.110	3137.4	16.147
274.006	835.7	20.231	327.963	3504.1	15.582
278.823	971.5	19.908	332.797	3901.7	14.955
283.645	1123.4	19.568	337.791	4349.4	14.175
288.530	1295.0	19.216			

233.15 K. The accuracy of the saturated vapor states is determined by two quantities, the accuracy of the vapor pressure and the accuracy of the virial surface. The accuracy of the low-temperature vapor pressure measurements was limited by the variation of the temperature for the glass

comparative ebulliometer. During each measurement the variation was 0.003 K above 220 K. This propagates to a relative uncertainty of the vapor pressure of 0.01% from 220 to 230 K. The variation of the temperature for the steel ebulliometer that was used by Weber and Silva (11) was 0.006 K between 230 and 270 K. The uncertainty of the pressure measurement is 0.03%. This resulted from the uncertainty of the vapor pressure of the reference fluid R123. The total uncertainty of the vapor pressures of R32 in this range is 0.05%. In all cases, the accuracy was not limited by the accuracy of the thermometer. Above 270 K, the pressures were measured using a static method, where the uncertainty was 0.1 kPa + 0.0002P. The uncertainty was then 0.03% at 270 K and 0.02% at 340 K. The correlation of the vapor pressure measurements represents the data to 0.03% in pressure. We have chosen to assign an uncertainty of 0.04% in the vapor pressure over the entire range of measurement.

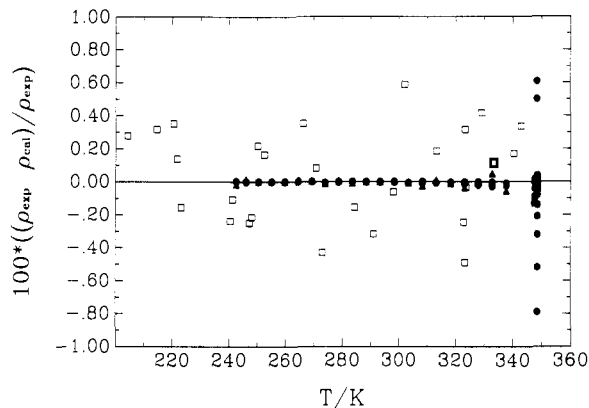


**Figure 4.** Density deviations from the mBWR correlation; this work, saturated liquid ( $\blacktriangle$ ), compressed liquid ( $\bullet$ ), and the data of Malbrunot et al. (13) ( $\square$ ).

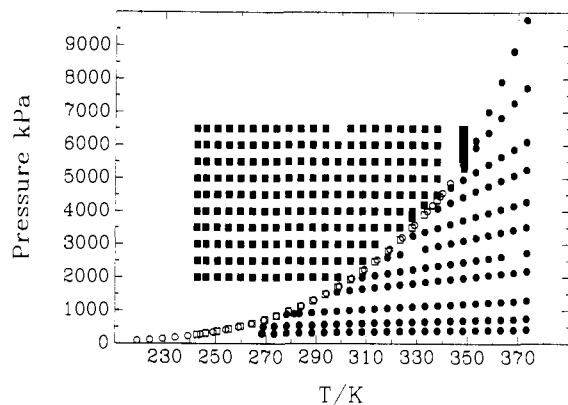


**Figure 5.** Location in pressure and temperature of the data used to derive tables: liquid PVT ( $\blacksquare$ ), vapor PVT ( $\bullet$ ), extrapolated saturated liquid densities ( $\square$ ), and extrapolated saturated vapor densities ( $\circ$ ).

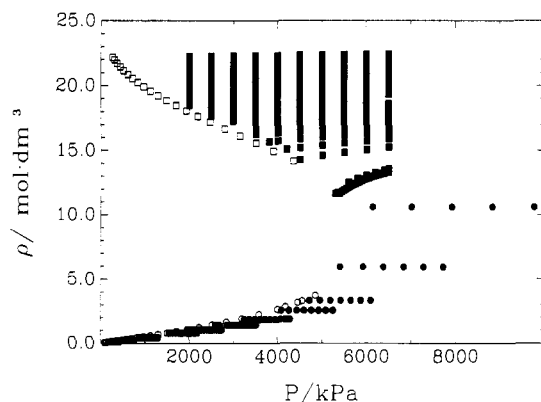


**Figure 6.** Location in density and pressure of the data used to derive tables: liquid PVT ( $\blacksquare$ ), vapor PVT ( $\bullet$ ), extrapolated saturated liquid densities ( $\square$ ), and extrapolated saturated vapor densities ( $\circ$ ).

The uncertainty in the second virial coefficient dominates the accuracy of the virial surface. The uncertainty in  $B$  is  $0.0005 \text{ dm}^3/\text{mol}$  at  $340 \text{ K}$ ,  $1.0\%$  at  $270 \text{ K}$ , and  $3\%$  at  $220 \text{ K}$ . The uncertainty in the first derivative of  $B$  is  $2\%$  at the highest temperature and increases to  $8\%$  at the lowest. For the second derivative of  $B$  the uncertainty increases from  $8\%$  to  $25\%$  as the temperature is reduced. The uncertainties in  $C$  are 10 times those for  $B$ , for  $D$ , 100 times those for  $B$ . The resultant uncertainty in the tabulated properties is noted below entries in the table at intervals of  $20 \text{ K}$ . As one would expect, the largest uncertainties are nearest the critical point where the virial expansion is least accurate. The enthalpy and entropy

**Table 7. Properties of R32 Ideal Gas**

$T/\text{K}$	$C_p^\circ / (\text{J}\cdot\text{mol}^{-1}\cdot\text{K}^{-1})$	$[S^\circ(T) - S^\circ(233.15 \text{ K})] / (\text{J}\cdot\text{mol}^{-1}\cdot\text{K}^{-1})$	$[H^\circ(T) - H^\circ(233.15 \text{ K})] / (\text{J}\cdot\text{mol}^{-1})$
200.00	36.695	-5.7554	-1244.77
205.00	36.937	-4.8464	-1060.73
210.00	37.190	-3.9531	-875.36
215.00	37.448	-3.0748	-688.72
220.00	37.716	-2.2110	-500.85
225.00	37.992	-1.3603	-311.56
230.00	38.275	-0.5221	-120.90
233.15	38.465	0.0000	0.00
235.00	38.567	0.3043	71.22
240.00	38.868	1.1194	264.83
245.00	39.176	1.9241	459.95
250.00	39.492	2.7188	656.62
255.00	39.815	3.5041	854.91
260.00	40.145	4.2805	1054.83
265.00	40.482	5.0484	1256.40
270.00	40.826	5.8084	1459.68
275.00	41.178	6.5607	1664.69
280.00	41.535	7.3059	1871.46
285.00	41.897	8.0443	2080.07
290.00	42.267	8.7764	2290.55
295.00	42.640	9.5019	2502.76
300.00	43.020	10.2217	2716.89
305.00	43.403	10.9362	2933.03
310.00	43.791	11.6450	3150.98
315.00	44.182	12.3490	3370.96
320.00	44.578	13.0480	3592.90
325.00	44.975	13.7423	3816.79
330.00	45.377	14.4320	4042.68
335.00	45.782	15.1174	4270.57
340.00	46.185	15.7988	4500.52
345.00	46.594	16.4759	4732.43
350.00	47.005	17.1493	4966.45
355.00	47.415	17.8192	5202.57
360.00	47.827	18.4852	5440.67
365.00	48.240	19.1478	5680.85
370.00	48.655	19.8069	5923.06
375.00	49.068	20.4628	6167.37
380.00	49.482	21.1156	6413.81
385.00	49.895	21.7651	6662.26
390.00	50.308	22.4116	6912.75
395.00	50.721	23.0552	7165.38
400.00	51.132	23.6960	7420.09

Vibrational Component with Respect to  $0.0 \text{ K}$  Ground State  
 233.15    5.207    1.6498    286.18

for the critical point were evaluated by fitting the mean for each of these quantities at the vapor pressure  $[(S_l + S_g)/2]$  and  $(H_l + H_g)/2$  to quadratic functions of the temperature and extrapolating them to the critical temperature.

Table 9 lists the saturated liquid volume, entropy ( $S$ ), and enthalpy ( $H$ ) as well as the entropy and enthalpy of vaporization. The reference state for this table is the same as for Table 8, and the uncertainty of the respective properties is noted at  $20 \text{ K}$  intervals. The accuracy of the liquid volumes is  $0.04\%$  except near the critical temperature. Density accuracy is limited by the ability of the densimeter to reproduce the density of the calibrating fluid water (8), and near the critical point, by the errors in the extrapolation of highly curved isotherms to the saturation boundary. The uncertainties in the entropy and enthalpy of the phase transition are determined by the uncertainty of the vapor volume, the vapor pressure, and the derivative  $d(\ln P)/d(1/T)$ . Over most of the temperature range the accuracy of the derived  $\Delta S_{\text{vap}}$  and  $\Delta H_{\text{vap}}$  is  $0.2\%$ . Only near the critical point, where there is considerable uncertainty in the vapor volume, does the uncertainty rise to several percent. The accuracies of the liquid-state entropies and enthalpies are determined by the uncertainties in the saturated gas states and the phase transition properties.

Table 10 lists the values of the different heat capacities at saturated liquid conditions. The quantity  $C_{\text{sat}} = \lim_{\Delta T \rightarrow 0}$

Table 8. Properties of R32 Saturated Vapor

T/K	P/kPa	V/(dm <sup>3</sup> ·mol <sup>-1</sup> )	S/(J·mol <sup>-1</sup> ·K <sup>-1</sup> )	H/(J·mol <sup>-1</sup> )	C <sub>p</sub> /(J·mol <sup>-1</sup> ·K <sup>-1</sup> )	C <sub>v</sub> /(J·mol <sup>-1</sup> ·K <sup>-1</sup> )
220.00	93.84	18.69	85.76	18 831.1	45.1	33.9
	(0.04)	(0.01)	(0.03)	(5.8)	(0.8)	(0.3)
225.00	120.75	14.744	84.33	18 958.8	46.4	34.8
230.00	153.45	11.763	82.97	19 081.0	47.9	35.7
233.15	177.41	10.259	82.16	19 154.8	48.8	36.2
235.00	192.79	9.480	81.69	19 197.4	49.4	36.6
240.00	239.63	7.713	80.47	19 307.6	51.1	37.6
	(0.10)	(0.005)	(0.04)	(10.2)	(1.2)	(0.4)
245.00	294.93	6.327	79.30	19 411.1	52.9	38.6
250.00	359.66	5.231	78.19	19 507.5	54.7	39.7
255.00	434.86	4.356	77.12	19 596.2	56.8	40.7
260.00	521.60	3.650	76.08	19 676.7	58.9	41.8
	(0.20)	(0.003)	(0.06)	(15.6)	(1.8)	(0.4)
265.00	621.00	3.076	75.08	19 748.2	61.3	42.9
270.00	734.23	2.606	74.12	19 810.0	63.8	44.0
275.00	862.49	2.218	73.17	19 861.1	66.6	45.1
280.00	1007.04	1.895	72.24	19 900.5	69.7	46.3
	(0.40)	(0.001)	(0.08)	(20.1)	(2.4)	(1.2)
285.00	1169.17	1.6253	71.32	19 926.8	73.1	47.4
290.00	1350.24	1.3980	70.41	19 938.8	76.9	48.6
295.00	1551.66	1.2053	69.50	19 934.3	81.2	49.8
300.00	1774.89	1.0411	68.58	19 911.5	86.2	51.0
	(0.70)	(0.0005)	(0.12)	(28.0)	(2.7)	(2.0)
305.00	2021.49	0.9002	67.64	19 867.6	92.1	52.3
310.00	2293.11	0.7787	66.67	19 799.1	99.2	53.5
315.00	2591.51	0.6710	65.66	19 701.7	108.0	54.9
320.00	2918.59	0.5809	64.59	19 569.5	119.2	56.2
	(1.20)	(0.0007)	(0.15)	(34.0)	(5.2)	(3.0)
325.00	3276.45	0.4996	63.44	19 394.1	134.1	57.7
330.00	3667.45	0.4274	62.17	19 163.4	155.1	59.2
335.00	4094.31	0.3622	60.74	18 857.7	187.2	60.9
340.00	4560.31	0.3023	59.03	18 440.4	243.5	62.8
	(1.8)	(0.013)	(0.30)	(54.1)	(78.6)	(5.6)
351.36	5792.7	0.1231	48.22	14 914	∞	∞
	(2.4)	(0.0008)	(0.66)	(165)		

Table 9. Properties of R32 Saturated Liquid

T/K	P/kPa	V/(dm <sup>3</sup> ·mol <sup>-1</sup> )	S/(J·mol <sup>-1</sup> ·K <sup>-1</sup> )	ΔS/(J·mol <sup>-1</sup> ·K <sup>-1</sup> )	H/(J·mol <sup>-1</sup> )	ΔH <sub>vap</sub> /(J·mol <sup>-1</sup> )
220.00	93.84	0.04 270	-4.73	90.48	-1076.4	19 907.5
	(0.04)	(0.00 002)	(0.21)	(0.18)	(45.8)	(40.0)
225.00	120.75	0.04 319	-2.91	87.24	-669.1	19 627.9
230.00	153.45	0.04 371	-1.12	84.09	-259.3	19 340.3
233.15	177.41	0.04 404	0.00	82.16	0.0	19 154.8
235.00	192.79	0.04 424	0.65	81.04	153.4	19 044.0
240.00	239.63	0.04 480	2.39	78.08	569.5	18 738.0
	(0.10)	(0.00 002)	(0.20)	(0.16)	(47.6)	(37.4)
245.00	294.93	0.04 539	4.11	75.19	989.5	18 421.6
250.00	359.66	0.04 600	5.81	72.37	1413.9	18 093.6
255.00	434.86	0.04 664	7.50	69.62	1843.1	17 753.1
260.00	521.60	0.04 732	9.17	66.92	2277.9	17 398.9
	(0.20)	(0.00 002)	(0.19)	(0.13)	(51.4)	(35.8)
265.00	621.00	0.04 803	10.82	64.26	2718.5	17 028.8
270.00	734.23	0.04 878	12.47	61.65	3165.6	16 644.4
275.00	862.49	0.04 959	14.11	59.06	3619.7	16 241.4
280.00	1007.04	0.05 044	15.76	56.50	4081.6	15 818.9
	(0.40)	(0.00 002)	(0.19)	(0.11)	(51.7)	(31.6)
285.00	1169.17	0.051 36	17.38	53.95	4551.8	15 375.0
290.00	1350.24	0.052 34	19.01	51.40	5031.4	14 907.4
295.00	1551.66	0.053 40	20.64	48.86	5521.0	14 413.4
300.00	1774.89	0.054 56	22.28	46.30	6022.0	13 899.5
	(0.07)	(0.000 02)	(0.21)	(0.09)	(55.8)	(27.8)
305.00	2021.49	0.055 84	23.93	43.71	6536.1	13 331.5
310.00	2293.11	0.057 25	25.59	41.08	7064.9	12 734.2
315.00	2591.51	0.058 84	27.28	38.38	7611.3	12 090.4
320.00	2918.59	0.060 64	29.00	35.60	8178.8	11 390.6
	(1.20)	(0.000 03)	(0.22)	(0.07)	(56.8)	(22.8)
325.00	3276.45	0.062 74	30.76	32.68	8773.0	10 621.1
330.00	3667.45	0.065 26	32.59	29.58	9402.0	9 761.5
335.00	4094.31	0.068 38	34.53	26.20	10079.9	8 777.8
340.00	4560.31	0.072 53	36.66	22.37	10834.6	7 604.8
	(1.8)	(0.000 05)	(0.97)	(0.67)	(264.0)	(210.0)
351.36	5792.7	0.123 1	48.22	0.00	14914	0.00
	(2.4)	(0.000 8)	(0.66)		(165)	

$T[S_{\text{sat}}(T_2) - S_{\text{sat}}(T_1)]/[T_2 - T_1]$  is calculated directly from the entropies in Table 9. To obtain  $C_p$  and  $C_v$ , standard

thermodynamic expressions (18) were employed. These require the derivatives at saturated liquid conditions:  $(d\rho/$

**Table 10. Properties of R32 Saturated Liquid Heat Capacities**

$T/K$	$P/kPa$	$V/(dm^3 \cdot mol^{-1})$	$C_{sat}$	$C_p/(J \cdot K^{-1} \cdot mol^{-1})$	$C_v$
220.00	93.84	0.042 70	80.9	81.0	46.0
	(0.04)	(0.000 02)	(1.5)	(1.6)	(3.2)
225.00	120.75	0.043 20	81.3	81.4	45.7
230.00	153.45	0.043 71	82.1	82.2	46.0
233.15	177.41	0.044 04	82.6	82.8	46.2
235.00	192.79	0.044 24	83.0	83.2	46.3
240.00	239.63	0.044 80	83.6	83.9	47.1
	(0.10)	(0.000 02)	(1.7)	(1.8)	(3.6)
245.00	294.93	0.045 39	84.2	84.6	46.3
250.00	359.66	0.046 00	85.6	85.4	46.4
255.00	434.86	0.046 64	85.9	86.5	46.7
260.00	521.60	0.047 32	86.8	87.5	46.8
	(0.20)	(0.000 02)	(1.8)	(1.9)	(3.8)
265.00	621.00	0.048 03	87.9	88.7	47.2
270.00	734.23	0.048 78	89.0	90.0	47.5
275.00	862.49	0.049 59	90.2	91.4	48.0
280.00	1007.04	0.050 44	91.5	92.9	48.6
	(0.40)	(0.000 02)	(2.0)	(2.1)	(4.0)
285.00	1169.2	0.051 36	93.0	94.9	49.1
290.00	1350.2	0.052 34	94.6	96.9	49.6
295.00	1551.7	0.053 40	96.3	99.1	49.9
300.00	1774.9	0.054 56	98.3	101.7	50.1
	(0.7)	(0.000 02)	(2.1)	(2.3)	(4.5)
305.00	2021.5	0.055 84	100.6	104.8	50.1
310.00	2293.1	0.057 25	103.1	108.4	50.3
315.00	2591.5	0.058 84	106.2	113.4	50.5
320.00	2918.6	0.060 64	110.0	118.7	51.0
	(1.2)	(0.000 03)	(2.2)	(2.9)	(5.2)
325.00	3276.5	0.062 74	114.7	126.4	51.8
330.00	3667.5	0.065 26	121.0	136.3	52.8
335.00	4094.3	0.068 38	130.0	143.4	55.2
340.00	4560.3	0.072 53	144.3	185.2	59.3
	(1.8)	(0.000 05)	(15.5)	(20.0)	(20.0)
351.36	5792.7	0.123 1	$\infty$	$\infty$	$\infty$
	(2.4)	(0.000 8)			

$dT)_{sat}$  from eq 4,  $d(\ln P)/d(1/T)$  from eq 3, and also  $(\partial P/\partial T)_v$  and  $P(\partial V/\partial T)_P/T$ , which were obtained by differentiating the PVT data numerically. We assign an uncertainty of 5% to the numerical derivatives, and this accounts for the greater uncertainties in  $C_p$  and  $C_v$ . As in Tables 8 and 9, the estimated uncertainties are noted at 20 K intervals.

### Summary

The PVT surface for R32 (difluoromethane) is deduced from data collected by a vibrating tube densimeter apparatus and a Burnett/isochoric apparatus. A vapor pressure equation is presented which has a relative standard deviation of 0.028% in pressure. A three-term virial surface correlates the vapor data and represents the vapor densities to 0.06% except at the lowest temperature. An abbreviated mBWR equation is used to correlate the liquid surface for the compressed liquid and saturated liquid densities. The saturated liquid data are

correlated and represented to 0.2% in density. Tables of heat capacities, enthalpies, and entropies at saturation are presented which were derived by a direct analysis of the PVT data.

### Acknowledgment

We thank Mark McClinden for providing software to evaluate the mBWR equation. We also thank Joe Magee for preliminary heat capacity data and L. A. Weber and A. M. Silva for vapor pressure data prior to their publication. This paper is dedicated in memory of Graham Morrison.

### Literature Cited

- (1) Scientific Assessment of Stratospheric Ozone. 1989 World Meteorological Organization Report No. 20; United Nations Environment Program, 1989.
- (2) Goodwin, A. R. H.; Morrison, G. *J. Phys. Chem.* **1992**, *96*, 5521.
- (3) Brand names and commercial sources of materials and instruments when noted are given for scientific completeness. Such information does not constitute a recommendation by the National Institute of Standards and Technology, nor does it suggest that these products or instruments are the best for the described application.
- (4) Bruno, T. J., NIST, Colorado. Personal communication, 1993.
- (5) Waxman, M.; Hastings, J. R. *J. Res. Natl. Bur. Stand.* **1971**, *75C*, 165.
- (6) Waxman, M.; Davis, H. A.; Horowitz, M.; Everhart, B. *Rev. Sci. Instrum.* **1984**, *55*, 1467.
- (7) Linsky, D.; Levelt Sengers, J. M. H.; Davis, H. A. *Rev. Sci. Instrum.* **1987**, *58*, 817.
- (8) Defibaugh, D. R.; Morrison, G. *J. Chem. Eng. Data* **1992**, *37*, 107-110.
- (9) Weber, L. A.; Goodwin, A. R. H. *J. Chem. Eng. Data* **1993**, *38*, 254-256.
- (10) Qian, Z.; Nishimura, A.; Sato, H.; Watanabe, K. The Compressibility Factors and Virial Coefficients of Difluoromethane (HFC-32) by a Burnett Method. Submitted for publication to *JSHE Int. J.*
- (11) Weber, L. A.; Silva, A. M., NIST Maryland. Personal communication, 1993.
- (12) Schmidt, J. W.; Moldover, M. R., NIST, Maryland. Personal communication, 1993.
- (13) Malbrunot, P. F.; Meunier, P. A.; Scatena, G. M. *J. Chem. Eng. Data* **1968**, *13*, 16-21.
- (14) Tait, P. G. *Physics and Chemistry of the Voyage of HMS Challenger*; Vol. II, Part IV, 1888 SP LXI.
- (15) Niesen, V. G.; Van Poolen, L. J.; Outcalt, S. L.; Holcomb, C. D. Coexisting Densities, Vapor Pressures and Critical Densities of Refrigerants R-32 and R-152a at 300K to 385K. Submitted for publication to *Fluid Phase Equil.*
- (16) Jacobsen, R. T.; Stewart, R. B. *J. Phys. Chem. Ref. Data* **1973**, *2*, 757-778.
- (17) Suzuki, I.; Shimanouchi, T. *J. Mol. Spectrosc.* **1973**, *46*, 130.
- (18) Rowlinson, J. S.; Swinton, F. L. *Liquids and Liquid Mixtures*; 3rd ed.; Butterworth Publishing: London, 1982; Chapter 2, pp 11-58.

Received for review July 29, 1993. Accepted November 15, 1993.\* This research project is supported in part by U.S. Department of Energy Grant Number DE-FG02-91CE23810 (Materials Compatibility and Lubricants Research (MCLR) on CFC-Refrigerant Substitutes) and in-kind contributions from the air-conditioning and refrigeration industry.

\* Abstract published in *Advance ACS Abstracts*, January 15, 1994.